

Supplementary Information for

Translational switching of Cry1 protein expression confers reversible control of circadian behaviour in arrhythmic Cry-deficient mice

Elizabeth S. Maywood*, Thomas S. Elliott, Andrew P. Patton, Toke P. Krogager, Johanna E. Chesham, Russell J. Ernst, Václav Beránek, Marco Brancaccio, Jason W. Chin, Michael H. Hastings* +

Elizabeth S. Maywood, MRC Laboratory of Molecular Biology, Neurobiology Division, Francis Crick Ave., Cambridge CB2 0QH. U.K. Tel: 0044 1223 267645. Email: emaywood@mrc-lmb.cam.ac.uk

Michael H. Hastings, MRC Laboratory of Molecular Biology, Neurobiology Division, Francis Crick Ave., Cambridge CB2 0QH. U.K. Tel: 00 44 1223 267045. Email: mha@mrc-lmb.cam.ac.uk

This PDF file includes:

Figs. S1 to S8

Supplementary Figure S1

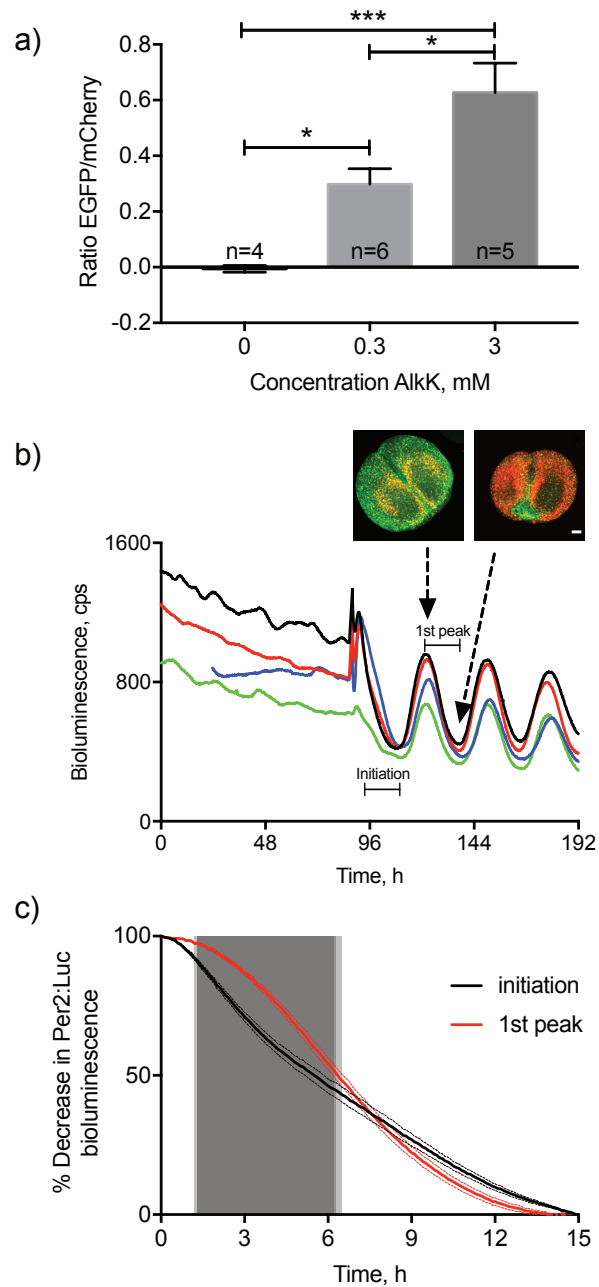


Figure S1. Control of cellular circadian rhythms by translational switching of *Cry1* expression in organotypic *Cry*-null SCN slices.

a) Expression of Cry1::EGFP relative to mCherry shows a dose-dependent increase, representing a dose-dependent increase in Cry1 expression. Mean \pm SEM ratio of EGFP to mCherry (n=4-6 SCN slices per dose) following addition of vehicle (0) or AlkK (0.3, 3mM) to the medium. In each slice the average, background subtracted ratio was taken from 40 cells over 2 fields of view (63x confocal image) (1xANOVA: F=16.95 df 2,12 p<0.001; post-hoc Tukey's multiple comparisons test *p<0.05 0.3mM AlkK vs vehicle; 0.3mM vs 3mM AlkK; ***p<0.001 3mM AlkK vs vehicle). b) Representative traces from 4 SCN slices treated with 1mM AlkK showing the decrease in the level of Per2::Luc bioluminescence following expression of pCry1-Cry1_(177TAG)::EGFP. Photomicrographs (x20; scale bar 100 μ m) show the colocalisation of Cry1::EGFP and mCherry (yellow/orange cells) at the peak but not at the trough of the Per2::Luc bioluminescence cycle c) Comparison between the mean (\pm SEM, dashed lines) decrease in bioluminescence recording from Cry1, 2-null Per2::Luc SCN slices (n=7) immediately following addition of 1mM AlkK ("initiation"; black line) and during the 1st TTF1-driven oscillation ("1st peak", red line). Grey bars represent significant differences between the "initiation" and "1st peak"; dark grey p<0.001; mid grey p<0.01; light grey p<0.05.

Supplementary Figure 2

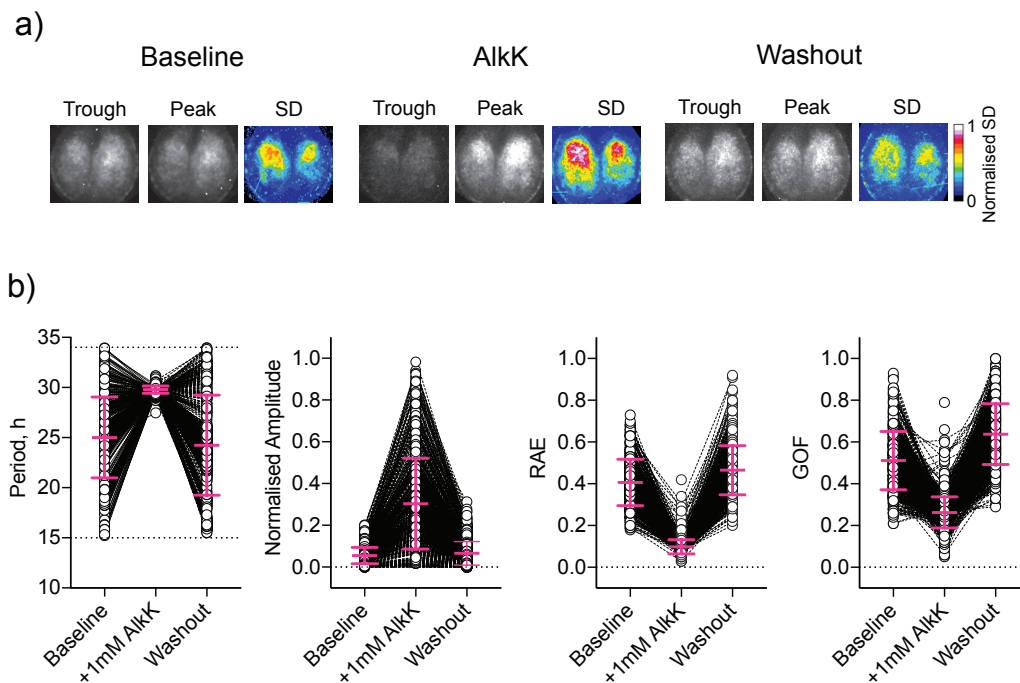


Figure S2. Control of cellular circadian rhythms by translational switching of *Cry1* expression in organotypic *Cry*-null SCN slices.

a) Representative pixel-based images of trough and peak bioluminescence, with corresponding standard deviation of signal over SCN during pre-AlkK baseline (left), during 1mM AlkK (centre) and following wash-out of AlkK (right) (images from Slice B). b) Corresponding FFT determined period, normalised amplitude, RAE (relative amplitude error) and GOF (goodness of fit) of cellular circadian oscillations from Slice B showing the coherence of the cellular rhythms during AlkK treatment but not during baseline or washout (mean \pm SD shown in magenta overlaid on top of the individual values).

Supplementary Figure S3

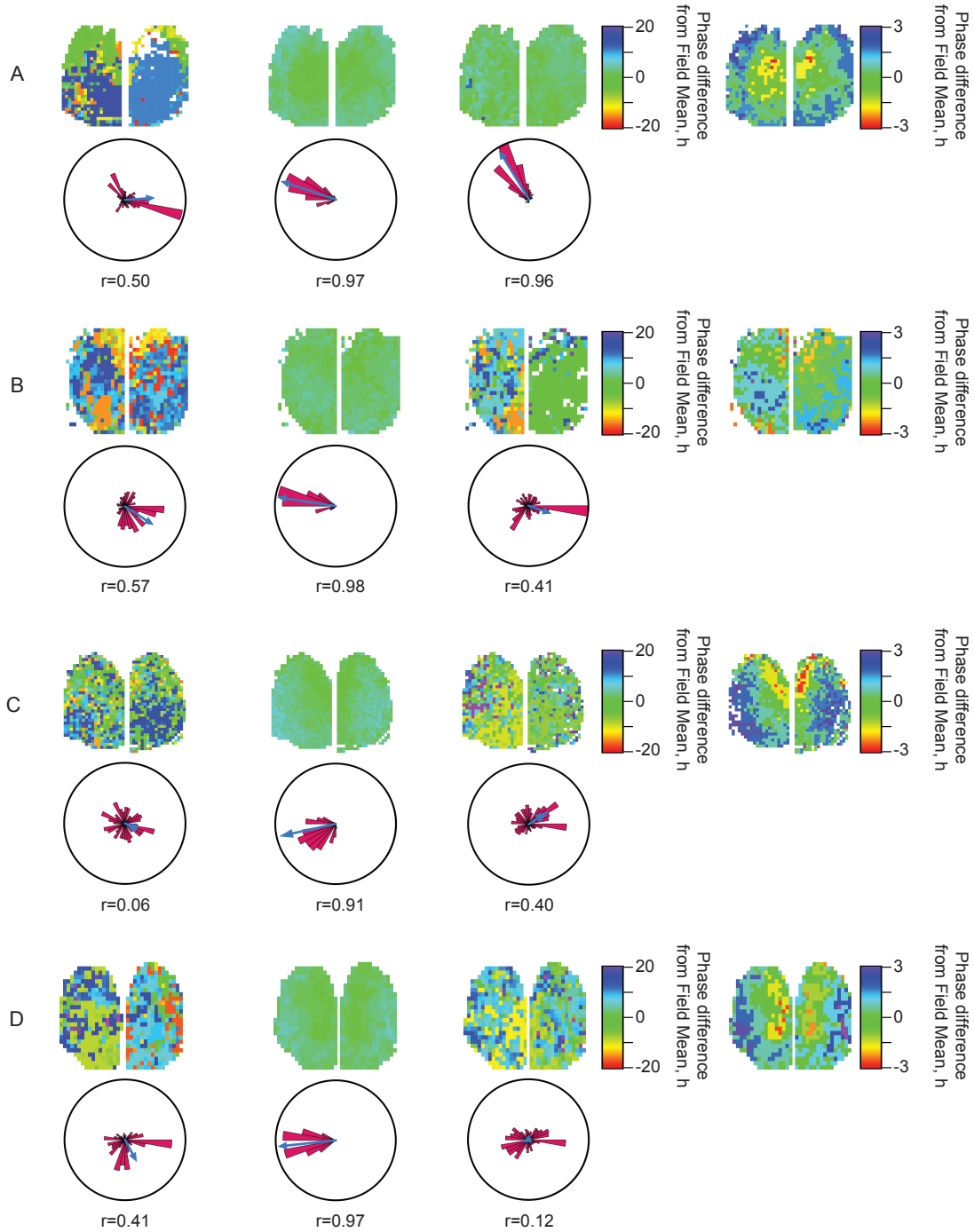


Figure S3. Control of circuit-level circadian organisation by translational switching of Cry1 expression in organotypic Cry-null SCN slices.

Phase distribution maps and associated Rayleigh plots from 4 independent Cry1, 2-null SCN slices (A-D) transduced with the AAV pCry1-Cry1_(177TAG)::EGFP. Data presented during the baseline (left), 1mM AlkK treatment (centre) and washout (right). Extreme right shows phase distribution during AlkK treatment but with an expanded scale (-3 to 3h vs -20 to 20h).

Supplementary Figure S4

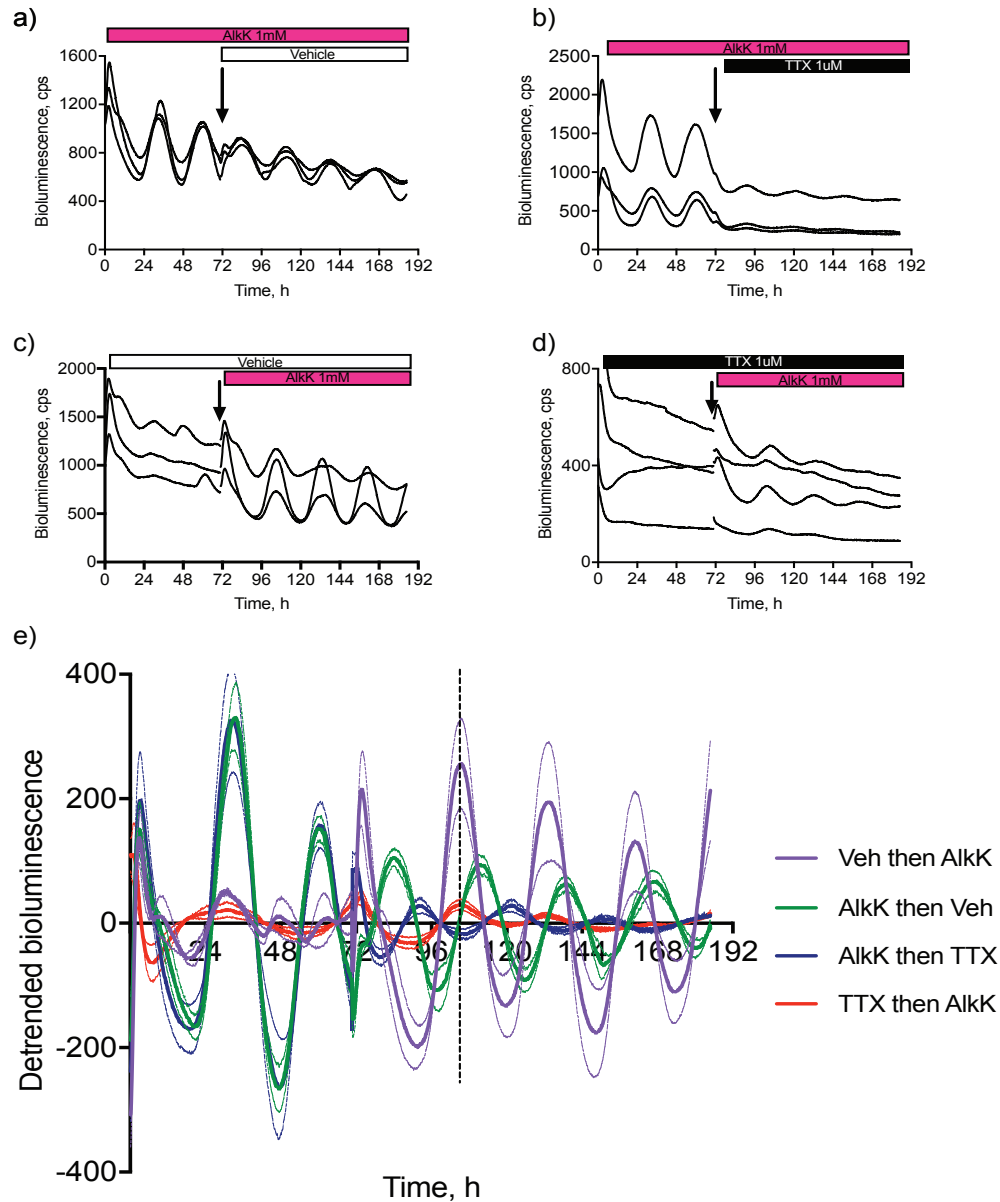


Figure S4. Control of cellular circadian rhythms by translational switching of Cry1 expression in organotypic Cry-null SCN slices is dependent on inter-cellular communication.

a) Per2::Luc bioluminescence traces from Cry1, 2-null SCN slices transduced with AAV pCry1-Cry1(177TAG)::EGFP and treated with 1mM

AlkK (magenta) followed by either vehicle or b) 1mM TTX (n=3/group). c) As in a) for slices treated with vehicle then AlkK (n=3), or d) TTX and then AlkK (n=4). e) Mean (\pm SEM, dashed lines) detrended bioluminescence traces from a) to d). The black dashed line aligns the 1st TTFL-driven peak following treatment with 1mM AlkK.

Supplementary Figure S5

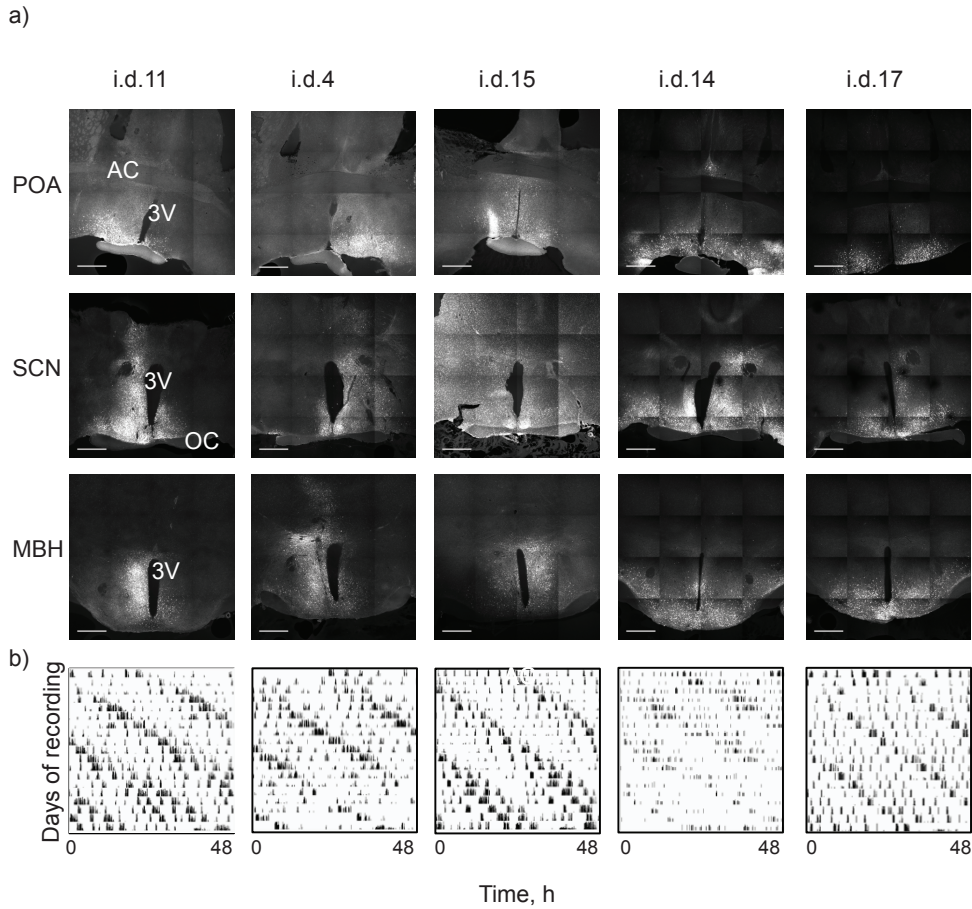


Figure S5. Translational switching of Cry1::EGFP expression in the SCN controls circadian behaviour of Cry1, 2-null mice.

a) Photomicrographs (20x magnification, 4x4 tiled) showing the rostro-caudal coronal distribution of Cry1_(177TAG)::EGFP expression in the hypothalamus of 5 representative Cry1, 2-null mice (3V: 3rd ventricle; AC: anterior commissure; OC: optic chiasm; POA: preoptic area; MBH: medio-basal hypothalamus) (Scale bar = 500µm). b) Representative double-plotted

actograms of wheel-running behaviour of the same mice as in (a) transferred to DD and provided with AlkK in drinking water. The traces are double-plotted on a 24h time base.

Supplementary Figure S6

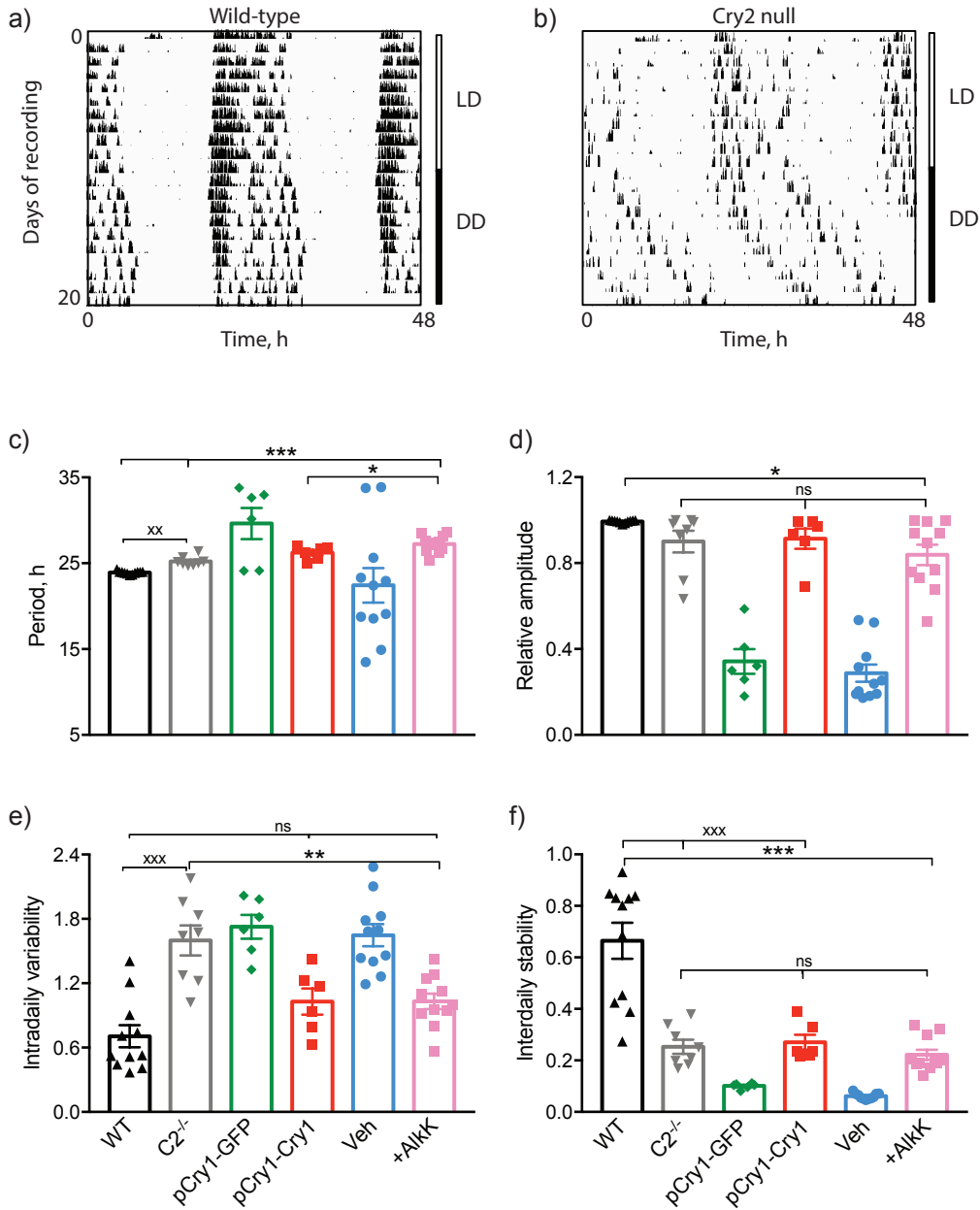


Figure S6. Quality and coherence of circadian behaviour initiated in Cry1, 2-null mice by translational switching of Cry1::EGFP expression in the SCN.

a, b) Representative double-plotted actograms of wheel-running behaviour of wild-type (a) or Cry2-null (b) mice. c- f) Group data (mean±SEM; n=6-11) for c) circadian period, d) non-parametric relative amplitude, e) intradaily variability and f) inter-daily stability of circadian wheel-running behaviour of wild-type (black; n=11) or Cry2-null mice (grey; n=8); or Cry1, 2-null mice injected with control AAV pCry1-EGFP (green; n=6) or non-conditional pCry1-Cry1::EGFP (red; n=6); or Cry1, 2-null mice injected with AAV encoding aminoacyl-tRNA synthetase/ tRNA_{CUA} pair, plus pCry1-Cry1(177TAG)::EGFP and treated with vehicle (light blue; n=11) or AlkK (magenta; n=11) for translational switching. (Period: post hoc Tukey's multiple comparison test *p<0.05 AlkK vs AAV pCry1-Cry1::EGFP; ***p<0.001 vs wild-type and Cry2-null; ^{xx}p<0.005 wild-type vs Cry2-null. Relative amplitude: 1xANOVA: F=3.2 df 3,32 p<0.05; post hoc Tukey's multiple comparison test *p<0.05 AlkK vs wild-type. Intradaily variability: 1xANOVA: F=12.1 df 3,32 p<0.0001; post hoc Tukey's multiple comparison test **p<0.005 AlkK vs Cry2-null, ^{xxx}p<0.0001 WT vs Cry2-null. Interdaily stability: 1xANOVA: F=22.4 df 3,32 p<0.0001; post hoc Tukey's multiple comparison test ***p<0.0001 AlkK vs wild-type; ^{xxx}p<0.0001 WT vs Cry2-null and AAV pCry1-Cry1::EGFP.).

Supplementary Figure S7

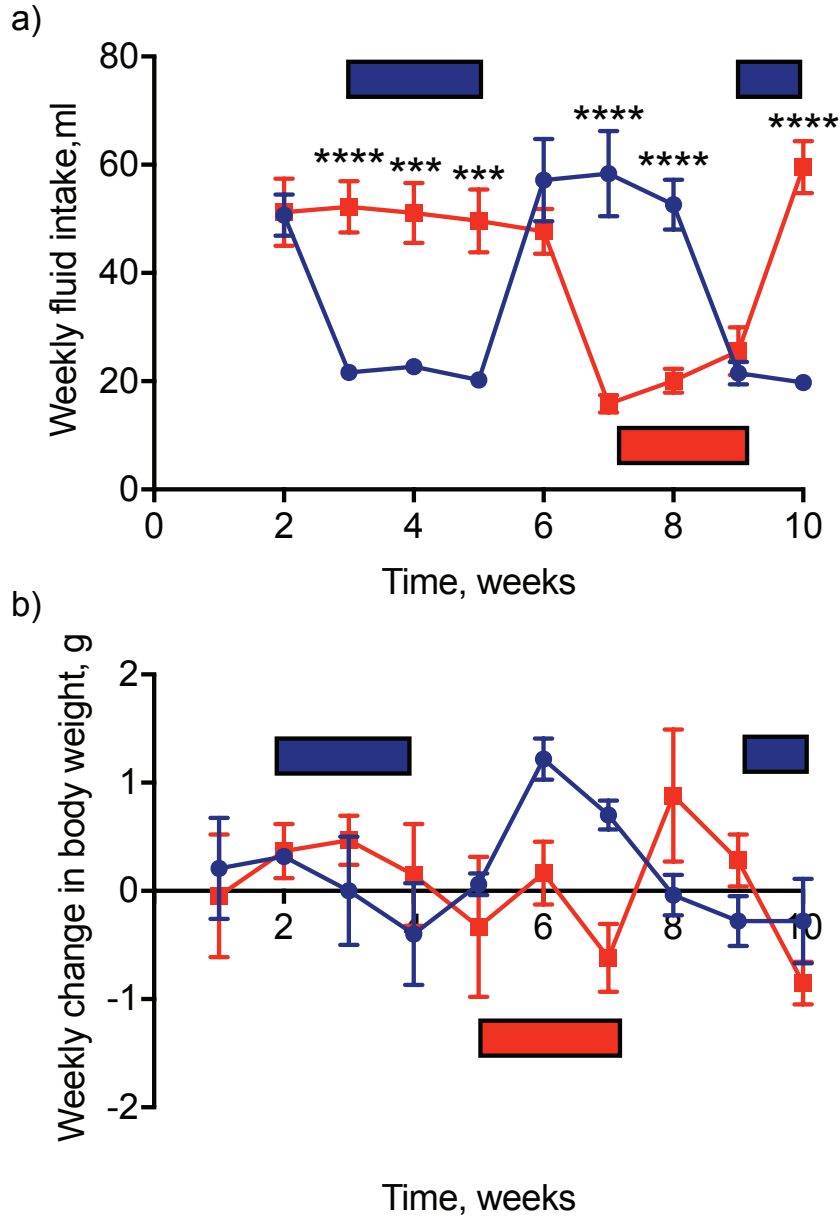


Figure S7. Effect of AlkK on drinking water consumption and maintenance of body weight.

a) Weekly fluid intake of Cry1, 2-null mice treated sequentially with AlkK, vehicle and AlkK (blue; n=5), or vehicle, AlkK and vehicle (red; n=6) in drinking water. Shaded blue and red blocks indicate phase of AlkK treatment. *** p<0.001 between groups (2xANOVA: Interaction F=55.0, df 8,75, p<0.0001; Time F=17.7 df 8,75 p<0.0001; Treatment F=2.0 df 1,75 p<0.05; post hoc Sidak's multiple comparisons test ****p<0.0001, ***p<0.001). b) Weekly change in body weight (mean±SEM), potted as in (a). (2x RM ANOVA: Interaction F=13.8, df 9,81, p=0.09; Time F=12.1 df 9,81 p=0.16; Treatment F=0.3 df 1,9 p=0.99).

Supplementary Figure S8

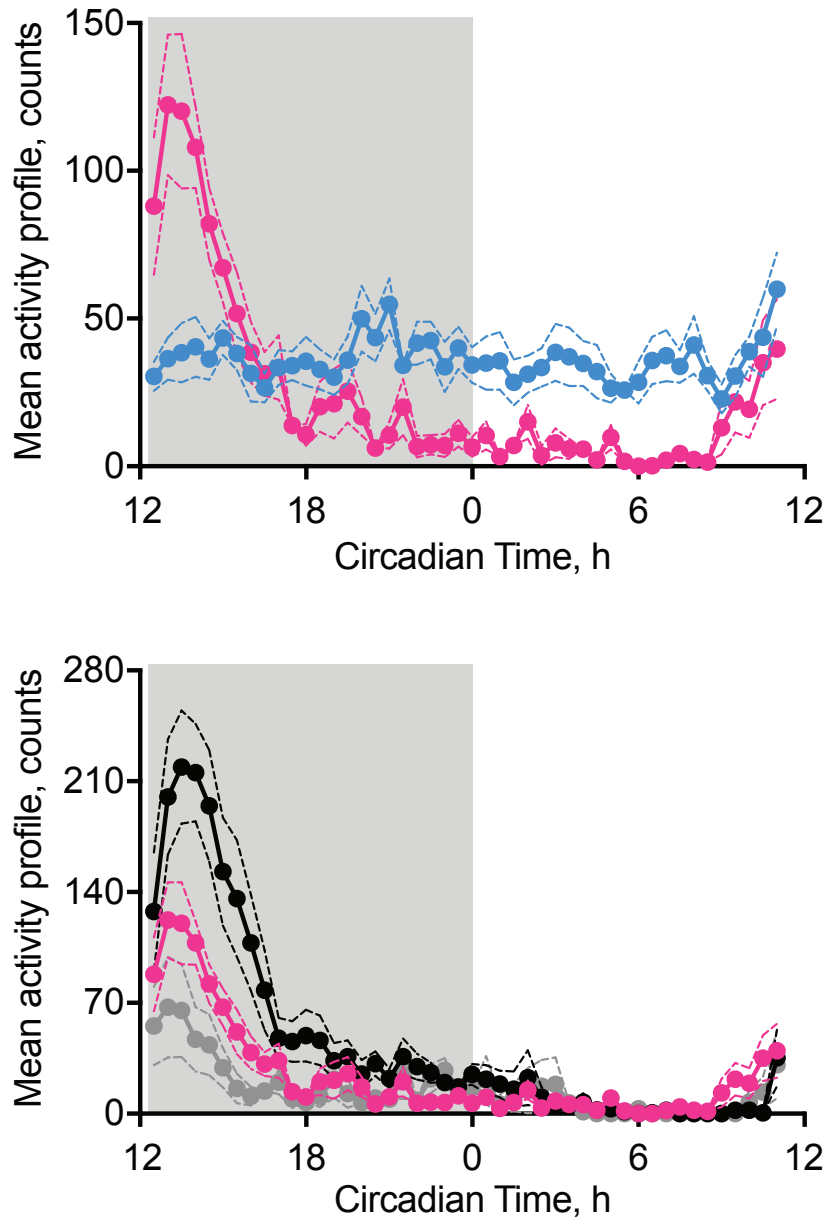


Figure S8. Comparison of circadian behavioural profiles of Cry1, 2-null mice undergoing translational switching of Cry1 expression and wild-type and Cry2-null mice.

a) Single-plotted group circadian activity profiles (mean \pm SEM, n =11/group) of AAV-injected Cry1, 2-null mice provided with vehicle (light blue) or AlkK (magenta) in their drinking water (Grey box denotes subjective night).

b) Circadian activity profile as in (a) for AlkK-treated mice (magenta, n=11), plotted alongside wild-type (black, n=11) and Cry2-null (grey, n=8) mice. (2xANOVA RM: Interaction F=12.5, df 90,1035, p<0.0001; Time F=32.4, df 45,1035, p<0.0001; Group F=4.5, df 2,23, p<0.005).